Solar Neutron Decay Protons observed in November 7, 2004

Yasushi Muraki (muraki@isee.nagoya-u.ac.jp)
ISEE, Nagoya University https://orcid.org/0000-0003-1978-2092
Jose F Valdes Galicia
Instituto de Geofisica, UNAM
Ernesto Fragoso Ortiz
Escuela Nacional de Ciencias Tierra, UNAM
Yutaka Matsubara
ISEE Nagoya University
Shoichi Shibata
Chubu University: Chubu Daigaku
Takashi Sako
Institute for Cosmic Ray Reserach, University of Tokyo: Tokyo Daigaku
Satoshi Masuda
ISEE, Nagoya University
Munetoshi Tokumaru
ISEE, Nagoya University
Tatsumi Koi
Faculty of Engeneering, Chubu University
Akitosi Oshima
Astronmy oBservatory, Chubu Unievrsity
Takasuke Sakai
Faculty of engennering, NihonUniversity
Tsuguya Naito
Yamanshi Gakuin Unievrsity
Pedro Miranda
U of T Physics: University of Toronto Department of Physics

Full paper

Keywords: Solar neutron decay protons, Solar flare, Solar Energetic particles, Particle acceleration

Posted Date: December 21st, 2020

DOI: https://doi.org/10.21203/rs.3.rs-131816/v1

Abstract

We have found an interesting event registered by the solar neutron telescopes installed at high mountains in Bolivia (5250m a.s.l.) and Mexico (4600m a.s.l.). The event was observed November 7th of 2004 in association with a large solar flare of magnitude X2.0. Some features in our registers and in two satellites (GOES11 and SOHO) reveal the presence of electrons and protons as possible products of neutron decay. Solar neutron decay protons (sndp) were recorded on board ISEE3 satellite in June 3rd, 1982. On October 19th, 1989, the ground level detectors installed in Goose Bay and Deep River revealed the registration of solar neutron decay protons (sndp). Therefore this is the second example that such an evidence is registered on the Earth´s surface.Key words: Solar neutron decay protons, Solar flare, Solar Energetic particles,Particle acceleration

1. Introduction

Gamma rays and neutrons propagate freely in the interplanetary medium when emitted as secondary products of solar explosion events. Therefore they may provide

information regarding the condition of production site and mechanism acceleration. Solar neutrons have been observed in space crafts and ground based detectors (see, e.g. Valdés-Galicia et al. 2009, Dorman 2010, Kamiya et al 2019, Muraki et al. 2020 and reference there in). In order to push forward this study, we have international solar neutron telescope (SNT) network at high mountains in the world. Evenson et al. (1983) reported the discovery of interplanetary protons by the decay of solar flare neutrons. Shea et al. (1991) found signals in neutron monitors for the event on 19 October 1989 that may be interpreted as the detection of relativistic protons that were the decay products of solar neutrons. Observing protons produced by the neutron decay in flight, very accurate energy spectra may be obtained. These spectra will be close to the source spectra.

In this paper we report registers obtained at two Solar Neutron Telescopes installed at high mountains, combined with the observations of two spacecrafts (GOES 11 and SOHO) that could be interested as products of the solar neutrons decay that were produced at the 7 November 2004 X2 solar flare.

The plan of the paper is as follows: in section 2 we give a brief description of the Solar Neutron Telescopes (SNT) at Bolivia and Mexico; section 3 is dedicated to a description of the observations in spacecrafts and on the Earth’s surface. In section 4 we give a plausible interpretation of the results. Then section 5 is dedicated to convert the fluxes observed on earth’s surface to fluxes on the top of the atmosphere to compare with the spacecraft observations. The sites where solar neutrons may have decayed are analyzed in section 6, to finish with our conclusions in section 7.

2. The Two Mountain Detectors Located On American Continent

Two solar neutron detectors are located at Mt. Sierra Negra (4,600 m, 19.0°N 97.3°W) and Mt. Chacaltaya (5,250 m, 16.3°S 68.1°W). The detector installed at Mt. Chacaltaya in Bolivia is comprised of 4 m^2 plastic

scintillator with 40 cm and the detector installed at Mt. Sierra Negra, Mexico is composed of the 4 m^2 plastic scintillator with 30 cm thickness. In addition, four layers of proportional counters are installed underneath the scintillator for the identification of the arrival direction of charged particles (Valdés-Galicia et al., 2004). These SNTs were constructed for the detection of solar neutrons. Both instruments distinguish neutral incidents from charged particles.

3. Main Features Of The Observed Events

 Signals recorded in the ground level detectors: increases of the counting rate were recognized in the 5-minute-value of the solar neutron telescopes (SNT) located in Bolivia from 15:48 to 16:06 UT, and in Mexico from 15:51 to 17:09UT. The statistical significance of each excesses was 3.7σ and 12σ respectively. Both data are shown in Figs. 1 and 2. The excesses of signal of the SNTs were observed almost at the same time, assuming them to be due to the solar flare of X2.0. Therefore, the increase cannot be explained by very plausibly originated at fluctuations of the background signal.

 Signals recorded in the detectors onboard the satellites: Fig. 3 shows the counting rate of the protons with > 10 MeV observed by the GOES11 satellite. An increase is apparently recognized between 15:50 UT and 16:00UT (16σ). An appropriate explanation on this bump is that the detector onboard the GOES11 satellite received solar neutron decay protons (sndp).

Figure 4 presents another candidate of neutron decay products detected by the electron detector COSTEP onboard the SOHO satellite that stays near the Lagrange point L1 (SOHO-COSTEP-EPHIN website). The excess was recorded by the COSTEP instrument during 15:58UT – 16:17UT. Solar neutron decay protons (sndp) were also observed by the COSTEP. In the proton channels 4.3–7.8 MeV and 7.8–25 MeV the excess of the sndp was clearly observed. However, in the highest channel 25–35 MeV, the excess was not definitely recognized. On the other hand, in the electron channels 0.25–0.70 MeV, 0.67-3.0 MeV and 2.64–10.4 MeV, the excess was clearly seen. These may be another evidence of neutron decay products via $n \rightarrow p + e^- + \nu_e$ process. Therefore neutron decay protons and electrons were observed not only inside but also outside of the magnetosphere.

4. Interpretations On The Event

We make the following hypotheses in order to explain the observations.

(**a**) The increase of the 5-minute counting rate registered during 15:48-16:07UT at Chacaltaya was induced by solar neutrons. These neutrons were produced by the impulsive flare with X2.0. One of the most probable production time was presumed when the derivative of the GOES X-ray intensity showed the first maximum at 15:47:00UT (Figure 5). Figure 5 shows that the flare reached X2.0 intensity via three step increase. The tendency is quite similar to a previous event observed in April 15, 2001 (Muraki et al. 2008).

(**b**) The increase of the counting rate observed between 15:51 and 17:09UT at Mt. Sierra Negra was produced by solar neutron decay protons (sndp) in the space between the CME front and the Earth. Here we specify the preceding CME as CME1. Since two large CMEs were produced: one in November 6^{th} at 00:34UT and another in 7^{th} at 16UT. Possible acceptable area for the sndp by each detector is pictorially shown in Figure 6. The distance D1 is estimated to be 10^7km.

First, the sndp produced near the magnetosphere arrived, then the sndp produced near the CME1 transported to the Earth. This is due to the fact that charged particles produced in the interplanetary space are transported toward the Earth along the inter-planetary magnetic field. That is one of the reasons why the excess of Mt. Sierra Negra continued for 78 minutes and was slightly delayed with respect to the neutron arrival time.

In comparison with the June 3^{rd}, 1982 even, the sndp of November 7^{th}, 2004 event was observed rather in a short period (~1/10). One of the reasons may due to the difference of decay space of the sndp by each detector. An explanation will be given in the next section.

The hypotheses (**a**) and (**b**) were introduced for two main reasons. One arises from the difference of the atmospheric thickness of the neutron path length between the two observatories. At the flare time, there were 200 g/cm^2 difference of atmospheric thickness between the two observatories for the passage of neutrons (Dorman et al., 1999, Tsuchiya et al. 1999, 2001). Therefore the flux at Mt. Sierra Negra should be 7 times less than that of Chacaltaya (~1/7), although both detectors are located at nearly the same altitude. (Let us remind that the Sun was situated above South America.) However, both excesses were detected with nearly the same intensity.

The second reason is based on the difference of the event duration. The signal of Chacaltaya was observed for 18 minutes, while the excess of Sierra Negra continued for 78 minutes (as shown by the horizontal arrow in Figure 2). Neutrons with 50 MeV energy are expected to arrive to the Earth 18 minutes later than the fastest neutron, if neutrons were produced. Neutrons with energy 50 MeV are possible to detect by the Chacaltaya detector, since the threshold energy is set at higher than >40MeV.

On the other hand, neutrons with the energy of 30MeV arrive at the Earth after 22 minutes (1,300 seconds) later than the highest energy neutron. The threshold energy of the Sierra Negra SNT was set at >30MeV. However, the increase continued for 78 minutes. Therefore it would be difficult to explain the signals observed at Mt. Sierra Negra by the direct hit of solar neutrons.

The excess of the counting rate at Chacaltaya was ~100 events/(m^2·minute) in the >40MeV channel between 15:48UT and 16:06UT. On the other hand, the S1 channel of Sierra Negra (the channel of charged particles with the energy higher than >30MeV) showed 133 events / (m^2·minute) as the excess between 15:51-16:27UT. The flux was observed with nearly the same intensity as that of Chacaltaya, and the excess start time was almost the same. However, the excess duration was completely different. Therefore, in order to explain both enhancements consistently, we may introduce the assumption that the

excess Chacaltaya was produced by the direct arrival of solar neutrons, while the excess Sierra Negra was produced by solar neutron decay protons (sndp).

We may take into account another effect for the estimation of the flux of the sndp, since the energy of sndp is expected to be around a few GeV. After transportation of

the sndp in the magnetosphere, some of them may be trapped by the Earth's magnetic field, but some of them will penetrate and arrive at Mt. Sierra Negra. The characteristic energy is called as the cut-off energy or Spörer limit (rigidity) for low energy protons. The cut-off energy of Mt. Sierra Negra and Mt. Chacaltaya are estimated as 3~4 GeV and 11~12 GeV respectively (Shea and Smart, 2000).

The differential energy spectrum of protons near the cut-off energy has been measured in space by PAMELA (2009, 2016) and AMS (2000) detectors independently. The result is shown in Figure 7 by the green triangles for the cut-off energy of 3-4 GeV. Therefore we will make an expected flux of sndp near the cut-off energy (the black circles in Figure 7), by multiplying the PAMELA's observed differential flux of 3-4 GeV (the green triangles in Figure 7) (Casolino 2007, PAMELA 2009) by the expected neutron energy spectrum of $E_n^{-4}dE_n$ (the red diamond in Figure 7). The energy spectrum of sndp beyond the cut-off energy is expected to reflect the neutron energy spectrum. However, in the low energy region less than the cut-off energy, the energy spectrum of sndp is predicted to have almost constant value to the neutron spectrum of $E_n^{-4}dE_n$. The magnetic latitude of the observatory is estimated as 30°N. The difference between the geographical latitude arises from the location of the magnetic-pole located at northern Canada (79°N) over ~260°E line (100°W line) in 2001.

(**c**) The increases observed by the GOES 11 satellite during 15:50-16:00UT (Figure 3) was also produced by the neutron decay protons. They were decay products of high energy neutrons in the energy range between 80 and 400MeV. If these neutrons were produced at 15:47UT, from the observed time, the parent neutrons had the energy between 80 and 400 MeV.

It may be interesting to know that the flux of neutron decay protons differs the two geostationary satellites. The increase was not observed in the detector onboard the GOES10 satellite. As for the longitude of both satellites on the Earth, the GOES11 was situated at 114°W, while the GOES10 was located at 135°W. In other words, the GOES11 satellite was located in the right above American continent (just over the longitude of Mexico City).

(**d**) Another bump of electron and proton components around 16UT was observed by the COSTEP instrument onboard the SOHO satellite (Figure 4). They were also produced by the neutron decays in the outer magnetosphere. Now we focus on the neutron decay electrons. Observation of electrons with energies higher than 2.64 MeV implies that initial neutrons should have a Lorentz factor γ=1.75 according to earlier predictions (Koi et al. 1993, Dorman 2010). It implies that original neutrons must have the kinetic energy higher than 700 MeV. So initial protons must be accelerated beyond 1 GeV at the impulsive

phase of the flare to produce high energy neutrons $E_n \geq 700$MeV. The kinematics of neutron decay protons and electrons is given in Appendix 1.

5. Flux Conversion Observed By The Ground Level Detectors To The Top Of Atmosphere

In order to compare each flux, in this section, we convert the flux measured by the ground level detectors to the top of the atmosphere.

a*) Deriving the flux of solar neutrons at the top of the atmosphere over Chacaltaya*.

In this section, let us derive the differential energy spectrum of solar neutrons at the top of the atmosphere. At 16UT (local time at 12LT), the atmospheric thickness over Chacaltaya is estimated as 550g/cm^2. The differential energy spectrum is derived with use of one-minute value of the counting rate of the channel with E>40 MeV of the solar neutron detector.

In order to derive the differential energy spectrum, we introduce the hypothesis that neutrons were produced impulsively at the solar atmosphere. The flight time of neutrons depends on its kinetic energy. We fixed the production time at 15:47:00UT. Then, the kinetic energy of neutrons is determined from the flight time (=arrival time – 15:47:00UT), so that the differential flux of solar neutrons is derived as a function of energy. The observed energy spectrum is given in Figure 8(a).

After we derived the observed energy spectrum of solar neutrons by the detector, we converted to the flux at the top of the atmosphere. For this purpose we used two correction factors, the detection efficiency of solar neutrons by the SNT (Watanabe 2005) and the neutron attenuation curve in the atmosphere (Shibata 1994). Combining these two correction factors into one curve, a correction curve is made. The results is shown in Figure 8(b) as a function of incoming neutron energy.

Dividing the energy spectrum observed at Mt. Chacaltaya (Figure 8a) by the correction curve (Figure 8b), finally the differential energy spectrum of solar neutrons at the top of the atmosphere of Chacaltaya has been derived. The differential energy spectrum at the top of the atmosphere is presented in Figure 8(c). The differential flux has been already normalized to the flux per unit area (/m^2).

b) *Flux of solar neutron decay protons over at Sierra Negra.*

Here we estimate the flux of the sndp over Mt. Sierra Negra. We use the observed results in space by PAMELA (2007, 2009) and AMS (2000). These results show that cosmic rays less energy than the cut-off energies have been observed. The green points of Figure 7 represent such effect. The events recorded by the Mt. Sierra Negra Solar Neutron Telescope between 15:51UT and 15:54UT may correspond to the highest of the solar neutron decay protons (sndp). Therefore, they may carry information on the flux near the cut-off energy of protons around E_{cut}~3GeV.

Incoming protons with energy about ~3 GeV make nuclear interactions with air nuclei. As a result, neutral pions are produced with an energy around ~1 GeV. These neutral pions immediately decay into two gamma rays and the gamma rays will make the electromagnetic cascade shower in the air. The tails of the cascade shower enter into the scintillator and gamma rays involved in the shower are converted into electrons and positrons. From the intensity of electron and positron signals, the arrival intensity of protons over Mt. Sierra Negra may be estimated.

Figure 7 (the black circles) suggests that the intensity of the sndp between E_p=1-3 GeV may be observed with an equal intensity and the spectrum is estimated to be flat. Therefore, we choose energy bin width (ΔE) of 3000MeV (=4000-1000MeV). Then we are able to estimate the differential flux of the sndp at 1-4GeV as (4.4±3.0) / (m^2.min.MeV) at the top of the atmosphere.

On the other hand the flux of solar neutrons at the top of the atmosphere over Mt. Chacaltaya is estimated as 12.8, 1.8, and 0.5 events/(m^2.min.MeV) at E_n=1, 2 and 3 GeV respectively. If we compare these numbers, the estimated solar neutron decay proton flux over Mt. Sierra Negra shows the Chacaltaya neutron flux. Given the assumptions made, we could say that the agreement is fairly good. Each flux is summarized in Table 1.

We are now preparing end to end simulation based on the GEANT4 code. In this simulation, the primary energy spectrum measured by the PAMELA detector and the attenuation of gamma rays in the atmosphere will be taken into account. We expect that with these simulations the error bars on the flux of sndp will be reduced. Furthermore if you look carefully to Figure 2, you may notice another enhancement: the counting rate of the anti-counter registering charged particles with energy higher than 30 MeV, and the lower detector located under the scintillator (L1 channel) indicate an increase from 18:00UT (14LT in Bolivia and 12UT in Mexico). It is possible that protons were further accelerated into high energies by the shock acceleration mechanism (Tsuneta and Naito 1998). We will discuss this matter in the next paper, together with the results obtained by the GEANT4 simulation.

6. Production Place Of Solar Neutron Decay Protons

Before we discuss the production place of sndp in the interplanetary space, let us summarize the general situation of the interplanetary space around 16UT on November 7th 2004. Around the flare time, a very short gamma ray burst was observed by the gamma ray burst monitors onboard INTEGRAL and WIND satellite (INTEGRAL web site, WIND web site). According to INTEGRAL SPIACS data, a very short gamma ray burst was recorded at 15:49:30 UT. The KONUS detector onboard the WIND satellite also detected the short gamma ray signal and they detected 2.2 MeV line gamma rays. The 2.2 MeV line gamma rays are emitted when a neutron is captured by a proton and to form a deuterium. The RHESSI satellite detected hard X-rays after 16:05 UT. In Figure 9, we present two images of the flare at a5:36 UT and 15:48UT. The images were taken by an ultraviolet telescope onboard SOHO. Within 16 minutes, an arch was emphasized in the image at 15:48UT. It is shown by the white artificial arc in the left side of Figure 9. Particles may possibly be accelerated within this arc.

Now let us describe briefly the characteristics of the CME1. According to the magnetometer measurement onboard ACE satellite (ACE web site) that stays at the Lagrange point L1, the maximum field strength of the CME1 was 40nT. This first CME1 (on the right side in Figure 6) was produced by the M9.3 flare of November 6th, *not* by the X2.0 flare of November 7th. According to the IPS observation, the CME2 arrived on the Earth around 9UT of November 9th (Tokumaru 2013). The CME2 produced at 16UT is depicted near the Sun in Figure 6.

The CME1 was already expanded in the interplanetary space at 16UT on November 7. From the record of the ACE satellite, the diameter of the CME1 may be estimated. We estimated it as 1= 10^7 km. The width of the CME1 was calculated by multiplying the time (9,000 sec) by speed (1,150 km/sec). Then we can estimate the maximum momentum of charged particles that will be trapped inside the CME1. By putting the numerical values into a simple equation pc=300Hρ, as H=4×10^{-4} gauss, ρ= 0.5 ×10^{12} cm, we get pc=6×10^{10}eV=60 GeV. The value is quite high. In other words, low energy charged particles may be trapped by the “CME barrier”, so that neutron decay protons produced between the Sun and the CME1 could not arrive the detector located near the Earth. Therefore, the observed sndp must be produced in between the front side of CME1 and the Earth. This region is pictorially shown in Figure 6 as **D1**. (Drawing is not proportional to the actual distance. The direct line approximation of the decay path may be guaranteed by the preceding calculations, at least during 60 minutes (Sakai and Muraki 1993, Sakai et al. 1997).

We examine “another barrier” for charged particles. It is the wall produced by the magnetosphere. The length of the magnetic-sheath ℓ3 is estimated as ℓ3= 2.7×R_earth = 17,000 km = 1.7 ×10^9cm. The field strength is estimated as between 20 nT – 40nT. Therefore, we choose 30nT. Again, putting these values into the equation of pc=300Hρ, we will get pc= 15 MeV. This time, the threshold energy is quite low, however protons with the energy less than 15 MeV produced between the CME1 and the bow shock cannot penetrate inside the magnetosphere. In this case, the initial neutrons observed by the GOES detector had an energy between 80 - 400MeV. Therefore the decay products (sndp) between Ep=80 MeV and 400 MeV can penetrate the magneto-sheath. (For the reference, we provide the length of ℓ2 and ℓ4 as ℓ2=10^7km =0.066AU, and ℓ4= 56,700 km respectively. The flight length from the front edge of the CME1 to the mountain detector **D**1 is estimated as **D**1= 1×10^7km + 67,000km≈ 1×10^7km.)

In the events observed in 1982 June 3, the sndp were registered for almost 12 hours (Evenson et al. 1983, 1990), while in the present event the excess was observed only during 75 minutes. The difference may be due to the existence of the preceding CME (CME1). In the 1982 June 3rd flare, there was no preceding CME (Solar Geophysical Data website). However in the event of 1989 October 19th, the sndp were observed for 30 minutes and the signals of sndp were masked by the strong accelerated proton beam produced by the X13 flare (Shea et al. 1991).

7. Conclusive Remarks

We have here presented evidence corresponding to registers in two spacecrafts and two ground based detectors. Taken together, observations admit an interpretation that would be consistent with the observation of solar neutron decay protons.

Solar neutron decay protons were first reported in 1981 by Paul Evenson, Peter Meyer, Roger Pyle. Ruffolo and other researchers discussed solar neutron decay electrons and protons afterwards (Ruffolo 1991, Dröge et al. 1996). However, we do not know any report of this kind of events after that of 19, October 1989. To the best of our knowledge, there are only three early reports on the detection of neutron decay protons and electrons onboard satellites and one report of neutron decay protons by ground level detectors in October 19^{th}, 1989. The event of October 1989, was also discussed (Koi et al. 1993). So, present event may be the second case where neutron decay protons were registered by a ground-based detector. Further study is necessary to understand this phenomenon deeply. However, we wanted to publish this quick report to call community attention in the search of neutron decay protons and electrons.

Abbreviations

sndp: solar neutron decay protons; En: neutron energy; Ep: proton energy, p: momentum of charged particles [eV]; c; light speed; ρ; radius of charged particles [cm]

Declarations

Availability of data and materials

Data can shared on request to the authors.

Competing interests

The authors declare that they have no competing interests.

Funding

The Chacaltaya Solar neutron Detector has been constructed by the President (S. Hayakawa) budget of Nagoya University. We also acknowledge UNAM-PA`IIT partial support through grant IN-104115.

Author's contributions

YM, JFVG, YMa, SS, TSako, and TS have constructed the Mt. Sierra Negra Solar Neutron Telescope, while YMa, TSako, YM and PM constructed the Chacaltaya solar neutron detector. YM, JFVG, EO and SS have made the data analysis. SM and MT provided the solar image and solar wind data respectively. SS prepared Appendix 1. All members jointed discussions.

Acknowledgements

The authors acknowledge INAOE personnel and authorities for their continued support in providing the services needed to keep the Mt. Sierra Negra SNT functioning well. The authors express the acknowledgment to the staffs of physics department of UMSA, who have kept the Solar Neutron Detector located at Mt. Chacaltaya under good condition for 28 years. We express sincere thanks to the satellite teams; particularly SOHO (LASCO, COSTEP, and EIT instruments) and ACE satellites, who provided valuable data available from the web site. This work has been carried out, being based on the international solar neutron telescope (SONTEL) network data reserved in the storage system of ISEE, Nagoya University.

Author details

[1]Institute for Space Earth Environmental Research, Nagoya University, Nagoya 464-8601, Japan, [2]Instituto de Geofisica, UNAM, 04510, Mexico D. F., Mexico, [3]Escuela Nacional de Ciencias de la Tierra, UNAM. Ciudad de México. 04510. México, [4]Engineering Science Laboratory, Chubu University, Kasugai, Aichi 487-0027, Japan, [5]Astronomy Observatory, Chubu University, Kasugai, Aichi 487-0027, Japan, [6]Institute for Cosmic Ray Research, The University of Tokyo, Kashiwa, Chiba 277-8582, Japan, [7]Physical Science laboratory, College of Industrial Technologies, Nihon University, Narashino, Chiba 275-0006, Japan, [8]Department of Information Science, Yamanashi Gakuin University, Kofu 400-8575, Yamanashi, Japan, and [9]Department of Physics, UMSA, La Paz, Bolivia

References

*) ACE web site;

http:// www.srl.caltech.edu/ACE/ASC/DATA/level3/mag/ACECpec.cgi?LATEST=1

*) Alex A. (2018) Script Lecture PHY 432, Physics with muons: from atomic physics to Solid state physics (psi ch.) (Access is available from website)

*) AMS collaboration; Alearaz et al. (2000) Protons in near earth orbits. Physics Letters B 472:215-226 https://doi.org/10.1016/S0370-2693(99)01427-6

*) Burman R.L. and Smith E.S (1989) LA-11502-MS, Parametrization of Pion production and Reaction cross-section at LAMPF energies (Access is available from website.)

*) Casolino M et al. (2007) Two Years of Flight of the Pamela Experiment: Results and Perspectives. J. Phys. Soc. Jpn. Suppl. A 78:35-40,

Casolino et al. (2007) Observation of primary, trapped and quasi trapped particles with PAMELA experiment. Proceed. 30th ICRC (Merida) 1:709-712,

Also in the rapporteur talk by E.O. Flückiger (2007) Ground Level Events and Terrestrial Effects. Proceed. 30th ICRC (Merida) 6: 239-253

*) Dorman LI, Valdés-Galicia JF, Dorman VI (1999) Numerical simulation and analytical description of solar neutron transport in the Earth's atmosphere, Journal Geophysical Research 104 (A10): 22417-22426. Doi.org/10.1029/1999jA900182

*) Dorman LI, Dorman IV, and Valdés-Galicia JF (1997) Simulation of solar neutron scattering and attenuation in the Earth's atmosphere for different initial zenith angles. Proceed. 25th ICRC (Durban) 1:25-28

*) Dorman L (2010) Solar Neutrons and Related Phenomena (Springer). pp 374-377

doi: 10.1007/978-90-481-3737-4

*) Dröge W, Ruffolo D, and Klecker B (1996) Observation of electrons from the decay of solar flare neutrons. ApJ 464: L87-L90

*) Evenson P, Meyer P, and Roger Pyle K (1983) Protons from the decay of solar flare neutrons. ApJ 274:875-882

*) Evenson P, Kroger R, Meyer P, and Reames D (1990) Solar Neutron Decay Proton Observations in Cycle 21. ApJ Suppl. 73:273-277

*) INTEGRAL web site: https://www.isdc.unige.ch/integral/science/grb#ACS

*) Kamiya K, Koga K. Matsumoto H., Masuda S, Muraki Y., Tajima H, and Shibata S (2019) Solar Neutrons observed from September 4 to 10 2017 by SEDA-FIB, PoS (ICRC2019) 1150.

*) Koi T. et al.(1993) Prediction of electrons as decay products of solar neutrons. Proceeding of 23rd ICRC (Calgary) 3:151-154

*) Muraki Y., Matsubara Y., Masuda S., Sakakibara S., Sako T., Watanabe K., Bütikofer R., Flückiger E.O., Chilingarian A., Hovsepyan G., Kakimoto F., Terasawa T., Tsunesada Y., Tokuno H., Velarde A., Evenson P., Poirier J., and Sakai T. (2008) Detection of high-energy solar neutrons and protons by ground level detectors on April 15, 2001. Astroparticle Physics 29:229-242 Doi:10.1016/j.astropartphys.2007.12.007

*) Muraki Y. Valdés-Galicia JF, González LX, Kamiya K, Katayose Y, Koga K, Matsumoto H, Masuda S, Matsubara Y, Nagai Y, Ohnishi M, Ozawa S, Sako T, Shibata, S, Takita M, Tanaka Y, Tsuchiya H, Watanabe K, and Zhang JL (2020) Possible detection of solar gamma-rays by ground-level detectors in solar flares on 2011 March 7. Pub. Astron. Soc. Japan 72:1-17 Doi: 10.1093/pasj/psz141

*) PAMELA collaboration; N. De Simone et al. (2009) Comparison of models and measurements of protons of trapped and secondary origin with PAMELA experiment. Proceed. 31st ICRC (Lodz) icrc0795

Adriani et al. (2016) PAMELA's measurements of geomagnetic cutoff variations during the 14 December 2006 storm.

Space Weather 14 210-220 doi:10.1002/2016SW001364

*) Ruffolo D (1991) Interplanetary transport of decay protons from solar flare neutrons. Astrophysical Journal 388:688-698 Doi: 10.1086/170756

*) Sakai T. and Muraki Y. (1993) Solar neutron Decay Proton. Proceed of 23rd ICRC (Calgary) 3:147S. Website: articles.ads.abc.harvard.edu/pdf/1993ICRC….3..1475

*) Sakai T, Kato M, and Muraki Y (1997) Propagation of Solar neutron decay protons near the Earth. Geomag. Geoelectr. 49:1105-1113

*) Shea MA, Smart DF, Wilson MD, and Flückiger EO (1991) Possible ground-level measurement of solar neutron decay protons during the 19 October 1989 solar cosmic ray event. Geophys. Res. Lett. 18 **:** 829-832. Doi.org/10.1029/90GL02668

*) Shea MA and Smart DF (2000) Cosmic Ray Implications for Human Health. Space Science Review 93:187-205

*) Shibata S (1994) Propagation of solar neutrons through the atmosphere of the Earth. Journal of Geophysical Research 99**:** 6651-6665

*) SOHO CME catalog website: https://cdawweb.gsfc.nasa.gov

*)SOHO-COSTEP-EPHIN : http://www2.physik.unikiel.de/SOHO/phpeph/EPHIN.htm

*) Solar Geophysical Data web site: https://www.ngdc.noaa.gov/stp/space-weather/online-publications/stp_sgd/1982/sgd8212c.pdf

*) Tsuchiya H.et al. (1999) Detection efficiency of new solar neutron detector. Proceed. 26th ICRC (Salt Lake City) 7: 363

*) Tsuchiya H.et al. (2001) Arrival of solar neutrons from large zenith angle. Proceed. 27th ICRC (Hamburg) 8: 3056-3059

*) Tsuneta S. and Naito T (1998) Fermi acceleration at the fast shock in a solar flare and the inclusive loop-top hard X-ray source. APJL 67:495

*) Tokumaru, M (2013) Three-dimensional exploration of the solar wind using observations of interplanetary scintillation, Proceedings of the Japan Academy Ser. B, 89(2):67-79 doi:10.2183/pjab.89.67.

*) Valdés-Galicia JF, Muraki Y., Sako T, Musalem O, Huertado A, Gonzalez X, Matsubara Y, Watanabe K, Hirano N, Tateiwa N, Shibata S, and Sakai T (2004) An improved solar neutron telescope installed at a very high altitude in México. NIMA 535: 656-664 doi.org/10.1016/j.nima.2004.06.148

*) Valdés-Galicia JF, Muraki Y, Watanabe K, Matsubara Y, Sako T, Gonzalez X, Musalem O, Huertado A (2009) Solar neutron events as a tool to study particle acceleration at the Sun, Advances in Space Research, 43: 565-572.

https://doi.org/10.1016/j.asr2008.09.023

*) Watanabe K. (2005) Proceeding of the Cosmic-ray Research Section of Nagoya University **46**(2), pp1-249. Solar neutron Events associated with Large Solar Flares in Solar Cycle 23 (PhD thesis in English)

*) WIND web site: https://asd.gsfc.nasa.gov

Tables

Table 1

Observation target	Solar neutron decay protons (sndp)	Sndp (protons)	Solar neutrons (neutrons)
Station (altitude)	GOES11 satellite	Mt. Sierra Negra (4,600m)	Mt. Chacaltaya (5,250m)
Flux / (m^2.min.) (excess time)	Given in bellow (15:50-16:00UT)	133±23 (15:51-16:27UT)	100±27 (15:48-16:06UT)
Differential flux /(m^2.min.str.MeV.)	(1.56±0.17)×10^7 (>5MeV) (7.8±1.8)×10^5 (>10MeV)	4.4 (@ ≥1000 MeV)	1.1×10^4 , 1.2×10^3 , 5.72 (@100, 200, 1000 MeV)
Correction factor	Direct observation	~0.01	3×10^{-4} ~ 2.5×10^{-3} (>100MeV, >200MeV)
Statistical significance	16σ (>10MeV)	12σ	3.7σ

Table captions: Differential fluxes of the ground level detectors are converted into the fluxes at the top of the atmosphere. In this calculation, the acceptance of the ground level detector is assumed as 1 steradian. On the other hand, the flux of the GOES represents the integral value beyond >5 MeV and >10 MeV respectively. However, the unit is expressed by m^2.min, not by cm^2 sec.

Appendix

Appendix 1 —kinematics of neutron decay electrons —

Let us define the parameters that are used for the estimation of the highest energy of electrons from neutrons. Here m_n, m_p, and m_e represents the mass of neutron, proton, and electron respectively. E_p* and E_e* are the energy of proton and electron in the center of momentum system (in the neutron rest system). In this calculation, we take the neutrino mass zero. Now we study an extreme case; proton and neutrino are emitted backward, while electron is emitted forward. Then the electron energy in the center of momentum system is expressed by

$E_e^* = ((m_nc^2 - m_pc^2)^2 + m_e^2c^4)/(2*(m_nc^2 - m_pc^2))$. (1)

We know $(m_nc^2 - m_pc^2)$ =1.29 MeV and m_ec^2 =0.511MeV.

Putting these values in Equation (1), we get E_e^*= 0.746 MeV.

From $(P_e^*c)^2 = E_e^{*2} - m^2c^4$, and P_e^*c = 0.544 MeV.

The Lorentz transform is expressed as

$E_e = \gamma (E_e^* + \gamma\beta P_e^* c \cos\theta^*)$, (2)

where γ represents the Lorentz factor of incident neutron.

So the electron energy in the laboratory frame Ee can be expressed by

$E_e = \gamma (0.746 + \gamma\beta \times 0.544)$ MeV in case $\cos\theta^*$=1 (3)

The threshold energy of COSTEP detector onboard SOHO satellite is 2.64 MeV.

Therefore solving the equation, we will get the minimum Lorentz factor of solar neutrons (γ) by $2.64 = \gamma (0.746 + \gamma\beta \times 0.554)$. (4)

When we put γ=1.75 and β=0.821 in Eq. (4), we will get $E_e \approx 2.67$ MeV.

Let us provide another extreme case, i.e., the proton is emitted forward and the electron and neutrino are emitted backward. The maximum energy of the proton in the center of momentum system is expressed by

$E_p^* = (m_n^2c^4 + m_p^2c^4 - m_e^2c^4)/2m_nc^2$. (5)

Since $E_p^* = m_pc^2$ and $P_p^* \approx 0$, in Eq. (2), we put E_p^* instead of E_e^*, then we get

$E_p = \gamma m_p c^2 = (m_p/m_n)*E_n$ (6)

Therefore the proton emitted the forward direction takes almost all the energy (99.9%) of the neutron.

Figures

Figure 1

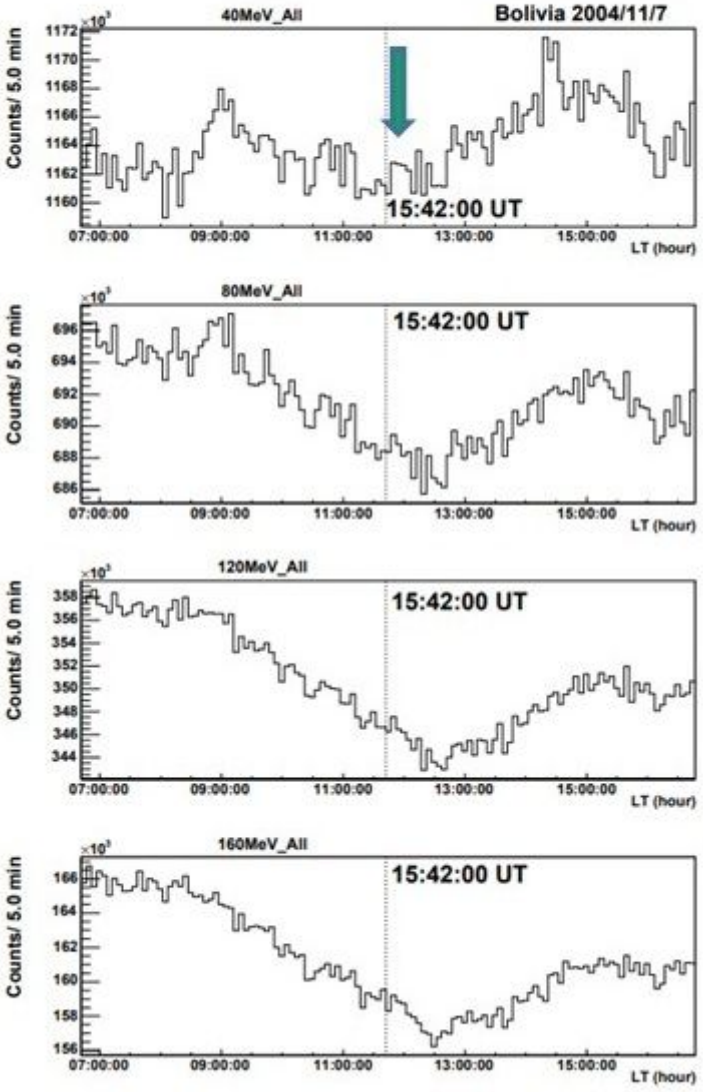

Figure 1

The 5-minute-value of the counting rate of the solar neutron detector located at Mt. Chacaltaya in Bolivia (5,250m a.s.l.). From top to bottom, it presents the counting rate of charged particles with the deposit energy higher than >40, >80, >120, and >160 MeV respectively. The threshold energy of the detector is calibrated by using the deposit energy of the minimum ionizing particles like muons. The arrow

corresponds to the time of the enhanced counting rate, around 16UT and the vertical dotted line represents the GOES flare start time. The horizontal presents the local time.

Figure 2 (5 minutes)

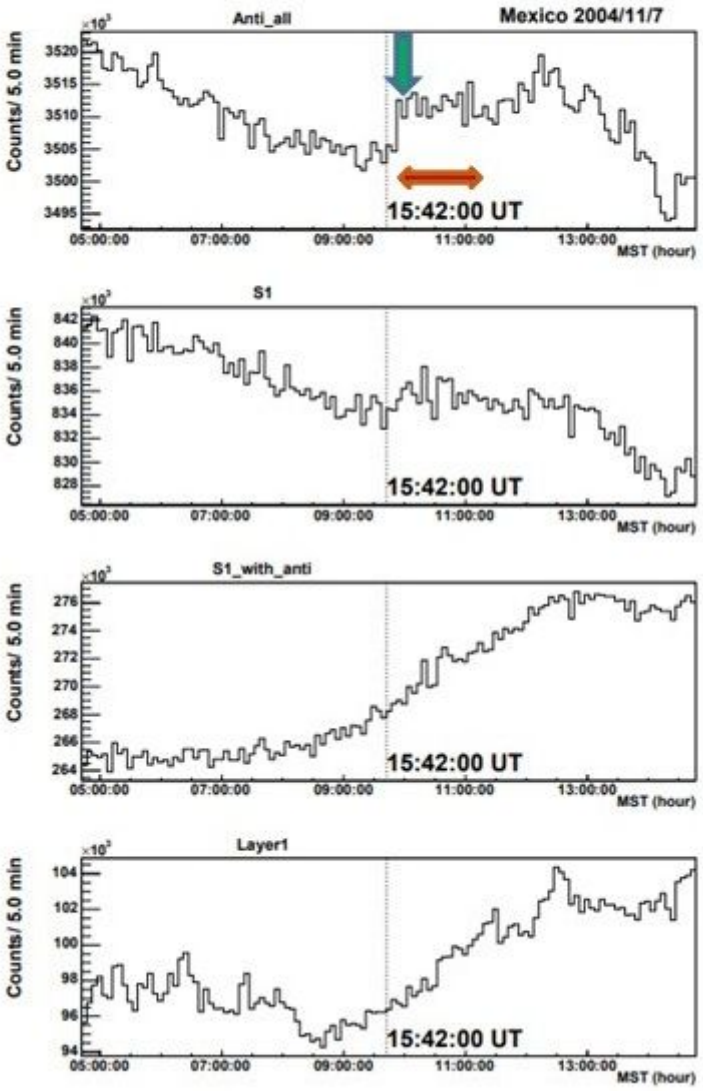

Figure 2

The 5-minute-value of the counting rate of the solar neutron telescope located at Mt. Sierra Negra in Mexico (4,600m a.s.l.). From top to bottom, the picture corresponds to the counting rate of all charged particles, charged particles with energy higher than 30 MeV, neutral particles with energy higher than 30 MeV, and the proportional counter located underneath the scintillator. We call it L1 channel (Layer 1). The L1 channel is triggered with the signal of S1 (>30MeV). The L1 channel is used for the identification of neutrons and gamma rays. The vertical dotted line presents the GOES flare start time (UT) and the horizontal arrow indicates the time of the enhanced counting rate.

Figure 3 GOES11 proton >10MeV

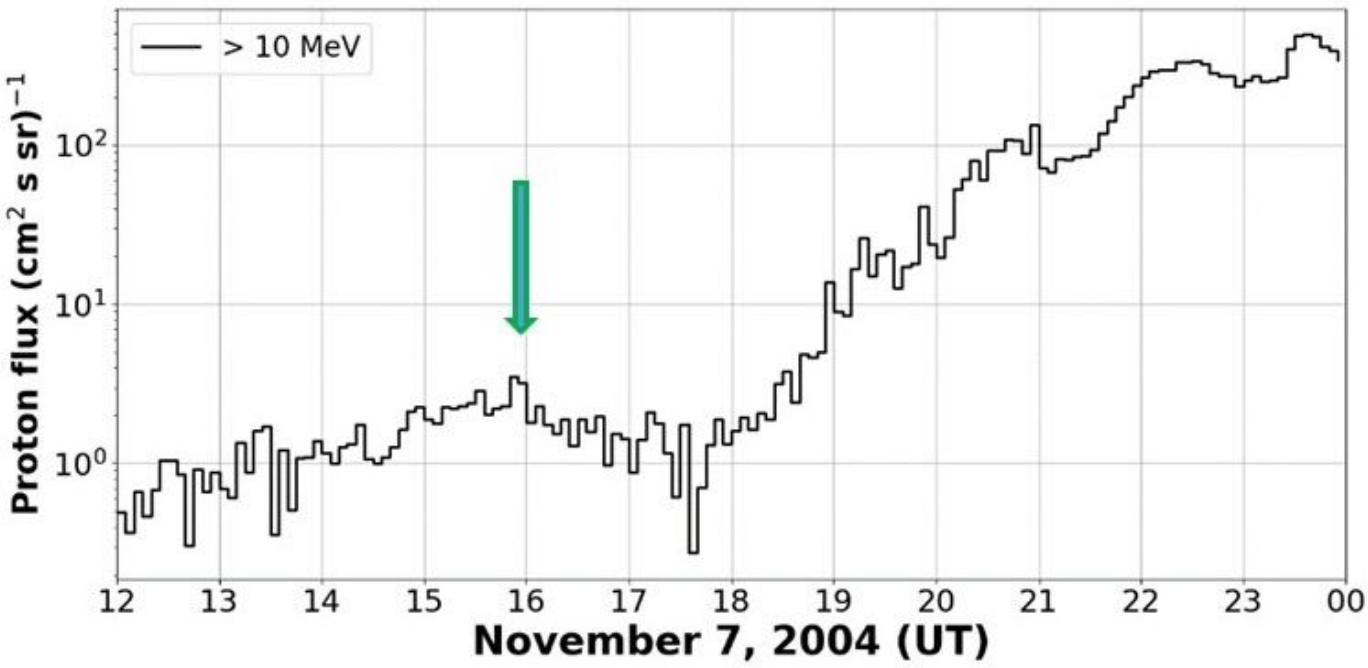

Figure 3

The time variation of the proton intensity with energy higher than 10 MeV measured by the proton counter onboard the GOES 11 satellite. An enhancement can be recognized 15:50-16:00 UT (indicated by an arrow). The enhancement corresponds to the impulsive phase of the solar flare X2.0 and may be produced by the neutron decay protons.

Figure 4 SOHO electron

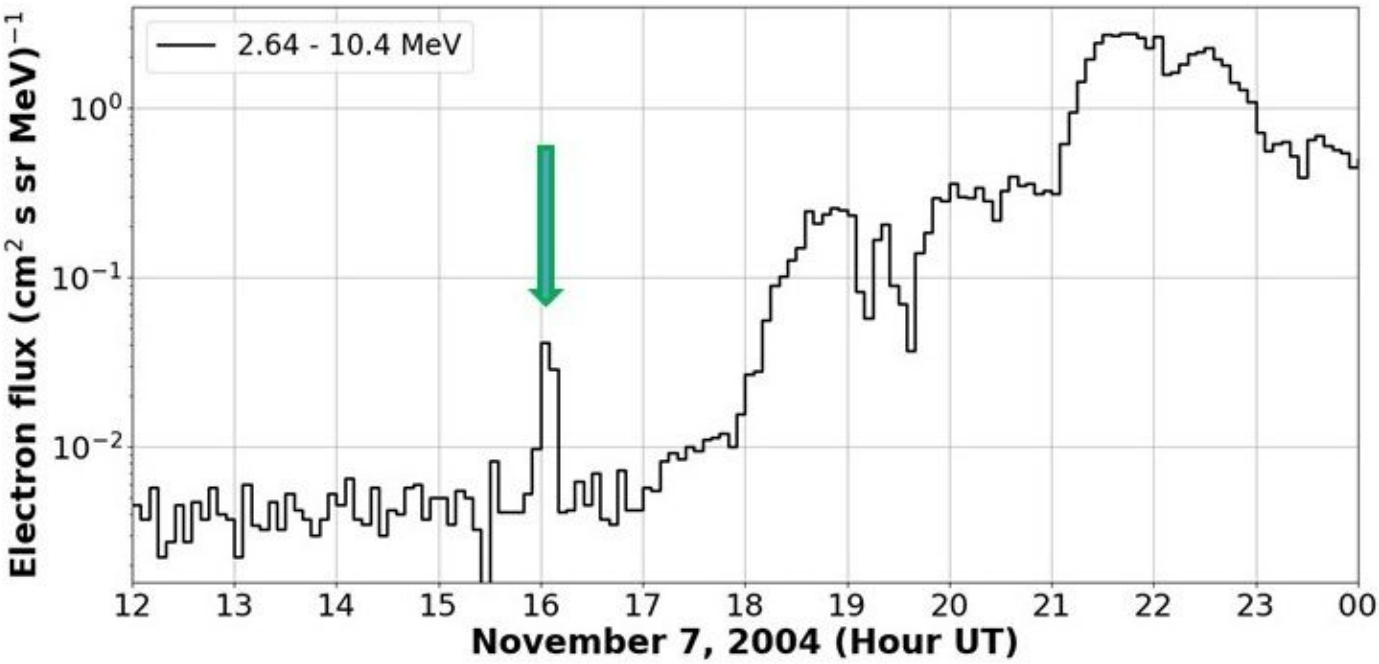

Figure 4

The time variation of the electron intensity with the energy 2.64-10.4 MeV measured by the COSTEP detector onboard the SOHO satellite. The enhanced time is indicated by the arrow. If the enhancement was produced by solar neutron decay electrons, the initial neutron should have the Lorentz factor $\gamma \geq 1.75$ according to Koi et al. (1993).

Figure 5 GOES 1-8Å, 0.5-4Å, derivative one minute value

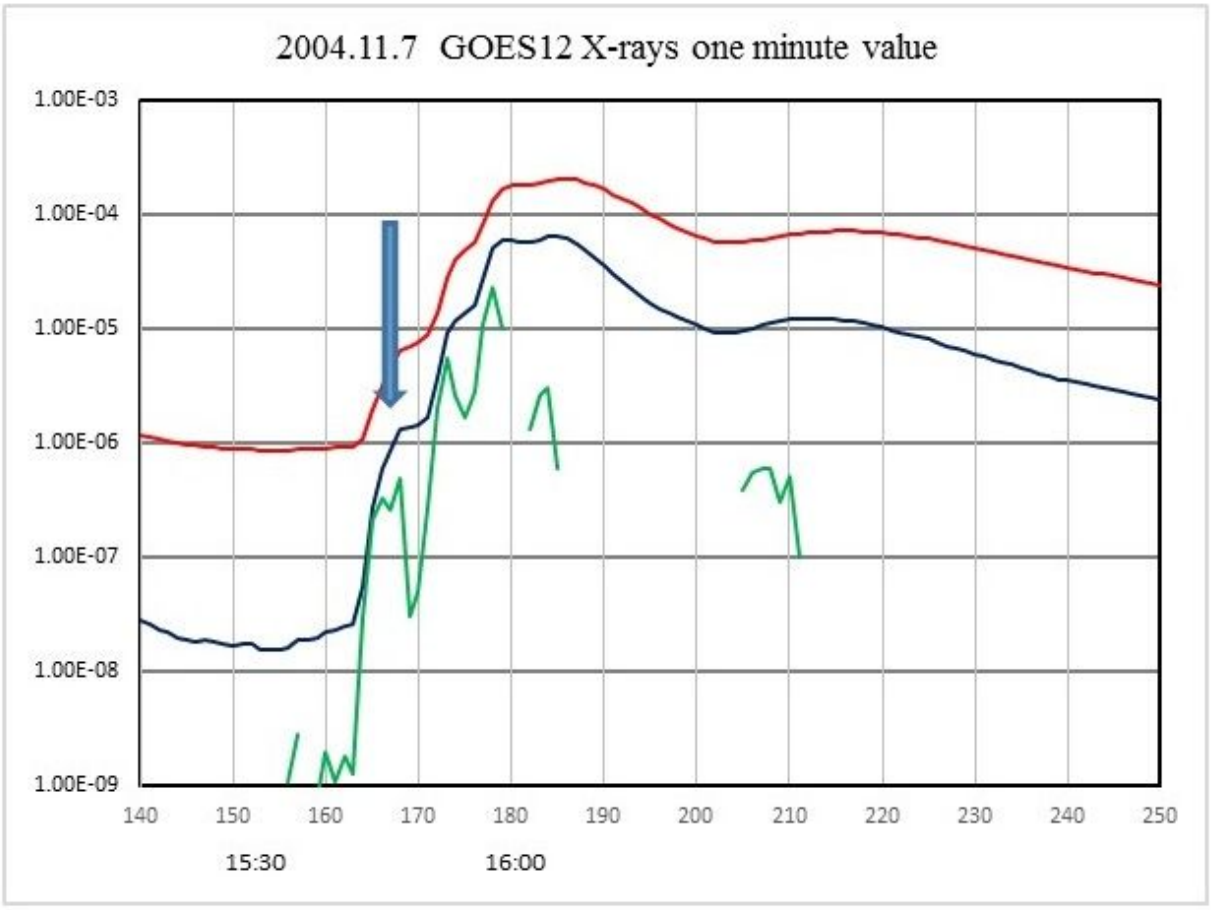

Figure 5

The one-minute time profile of GOES X-ray intensity from 15:20 UT to 17:10 UT November 7, 2004. The red line and the blue line correspond to the X-rays with the wave length 1-8Å and 0.5-4Å respectively. The green line represents the derivative of the short band of X-rays. We assume that neutrons were produced instantaneously at 15:47:00 UT, when there is a change of slope of the emission.

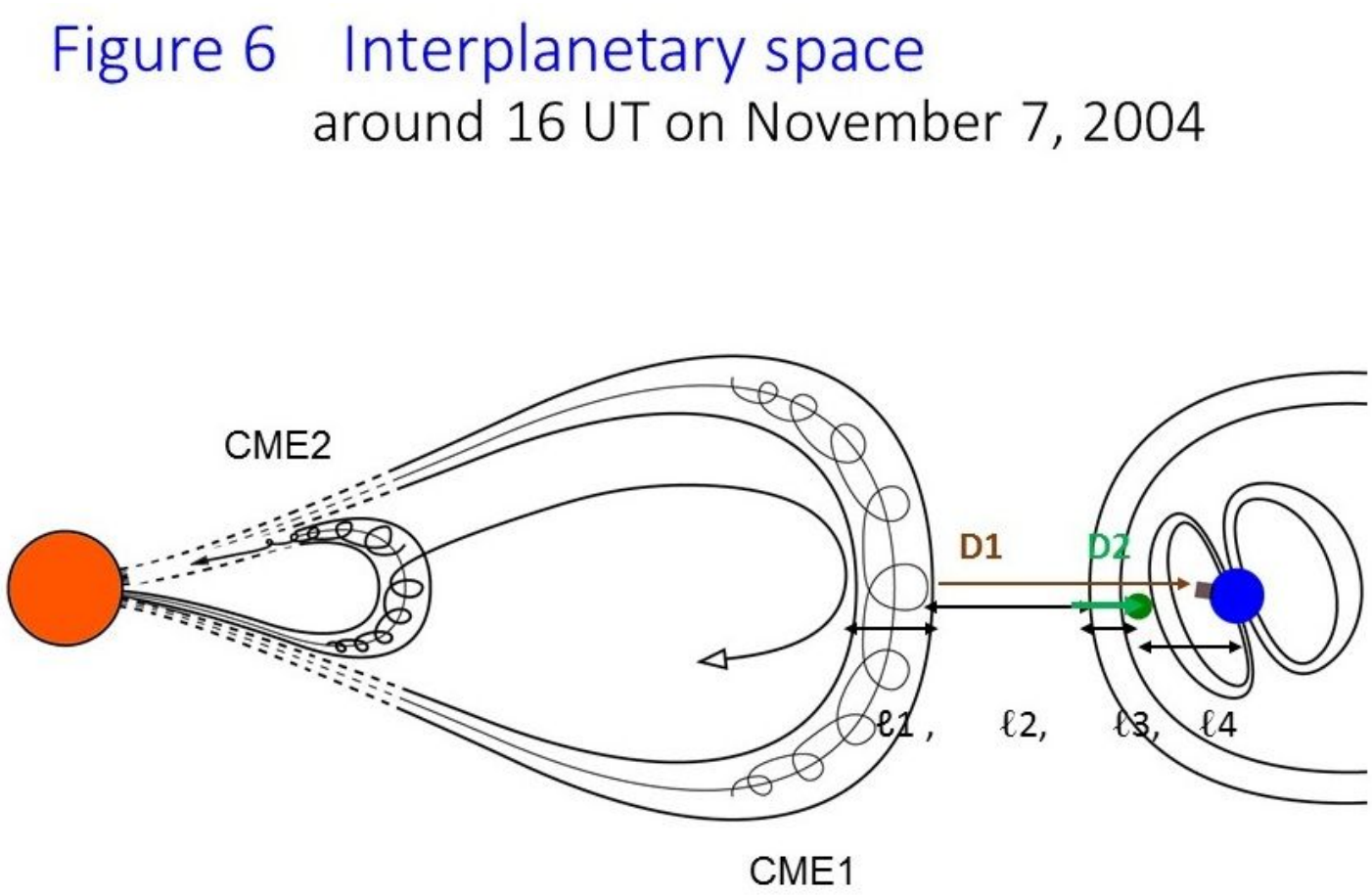

Figure 6

The interplanetary plasma scenario around 16UT of November 7th, 2004 is depicted. ℓ1 represents the width of the CME emitted at 00:34UT on November 6th flare. The front of CME had not yet arrived near the Earth at 16UT, situated about 1×107km (ℓ2) away from the (ℓ3) of the Earth. The front of the magnetosphere was extended at about 9R_earth (ℓ4). The green star presents the position of the GOES satellite and the brown mark corresponds to Mt. Sierra Negra observatory. D1 represents the distance from the CME front to the mountain laboratory, and D2 (=2.2×104 km) depicts the distance from the bow of the magnetopause to the GOES satellite.

Figure 7

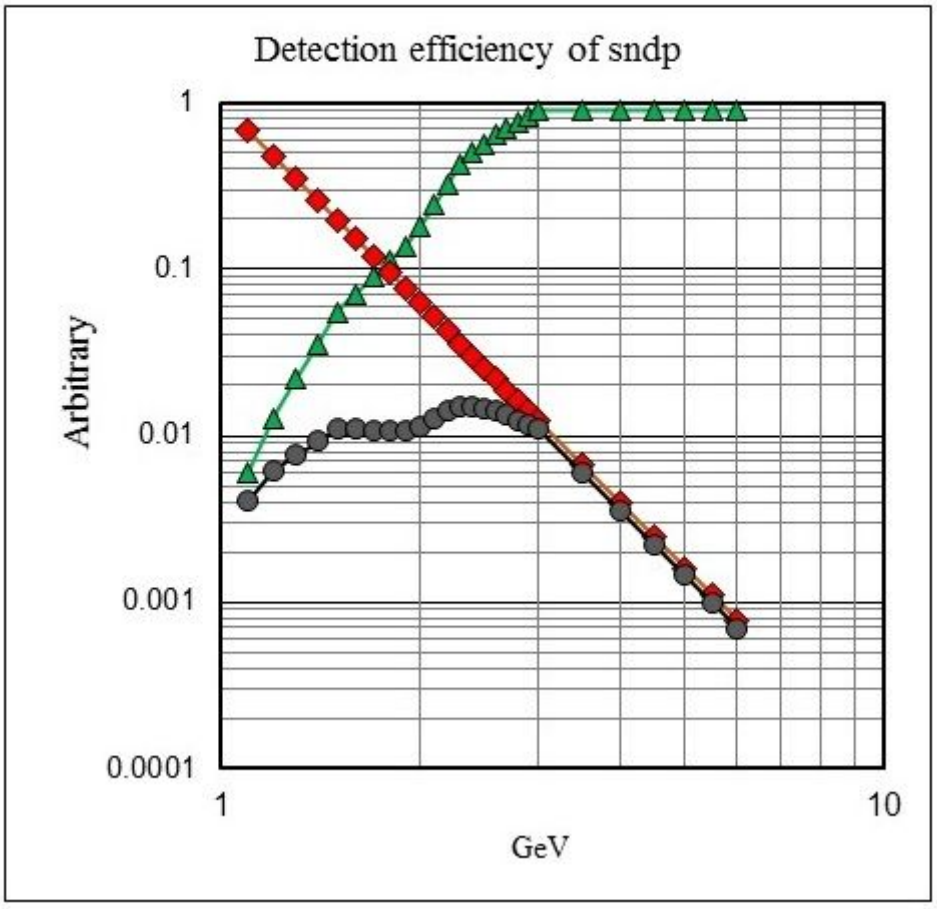

Figure 7

The expected solar neutron decay proton (sndp) flux at Mt. Sierra Negra (the black circles). The red diamonds represent a possible production spectrum of solar neutrons for the energy spectrum of En-4dEn. The green triangle presents the observed proton flux by the PAMELA detector near the cut-off energy of 3-4 GeV. Beyond the cut-off energy, the energy spectrum of the sndp represents the neutron spectrum.

Figure 8 (a) neutron energy spectrum

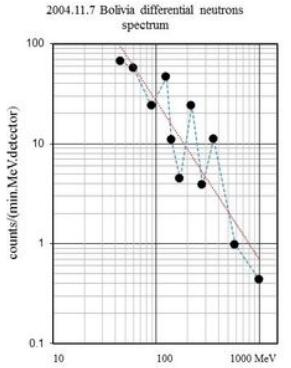

Figure 8(b) correction factor for solar neutrons

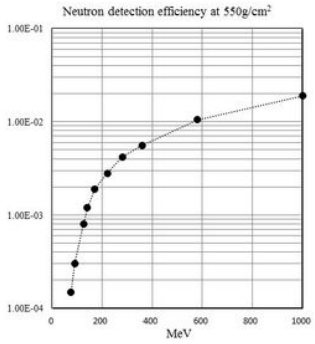

Figure 8(c)
Differential energy spectrum of solar neutrons observed in November7, 2004

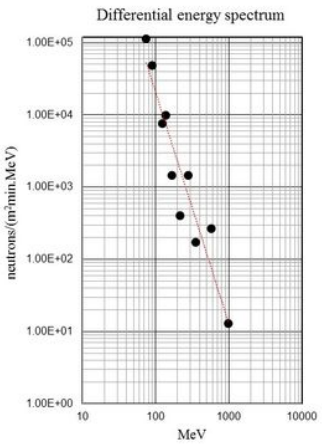

Figure 8

(a) the original energy spectrum observed at Mt. Chacaltaya, (b) the correction factor for the energy spectrum to the observed spectrum. The curve is made by folding the two correction factors; the detection efficiency of the counters and the attenuation of neutrons in the atmosphere. (c) The estimated energy spectrum at the top of the atmosphere over Mt. Chacaltaya in units of flux/(cm⁻²·min. MeV)⁻¹

Figure 9

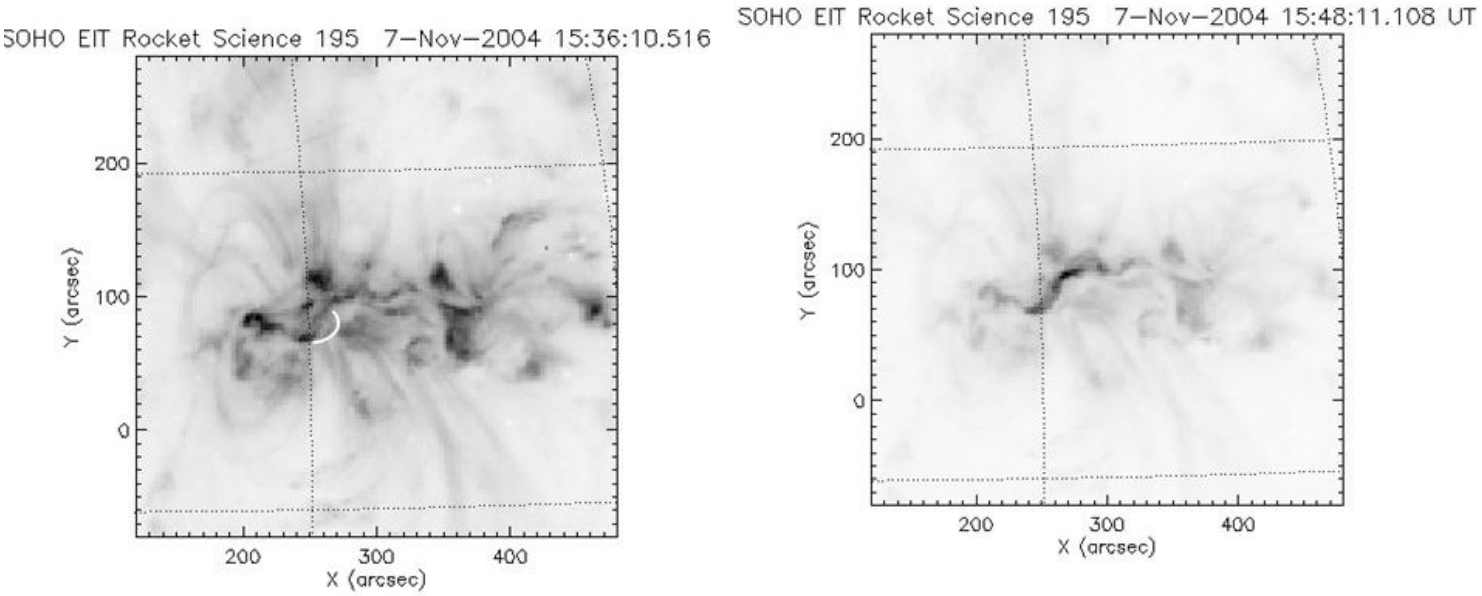

Figure 9

Solar images taken by the EIT telescope onboard SOHO satellite at 15:36 UT (left) and 15:48 UT (right). The UV wave length is 19.5nm. We assume that neutrons were instantaneously produced at 17:47UT. If you compare the two images (a) and (b), you will notice a plasma arcade in the image of 18:48UT. The

arc is shown by a white arc in the image of 15:36UT and possibly it had an important role for the particle acceleration.

Figure 10 Solar wind speed map derived from interplanetary scintillation (IPS) observations

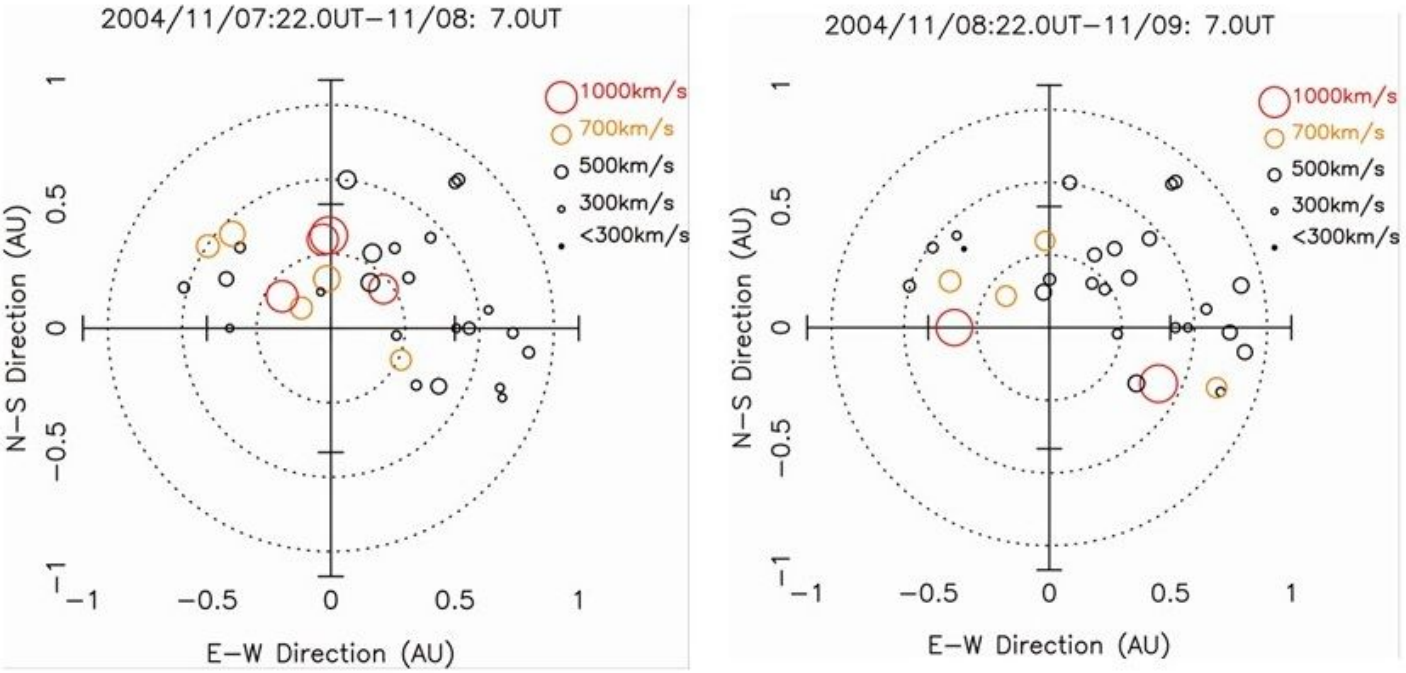

Figure 10

The sky projection maps of the solar wind speed derived from the observations of the interplanetary scintillation device (IPS) using the 327-MHz multi-station system of Nagoya University (Tokumaru, 2013). The data were accumulated during the periods (left side) between 22 UT of November 7, and 7 UT of November 8, 2004, and (right side) between 22 UT of November 8 and 7 UT of November 9, 2004 respectively. Four IPS antennas observed IPS for the same radio sources simultaneously. The solar wind speed was determined by detecting the time lag between the variations of the intensity at the separated stations. The center of the map corresponds to the location of the Sun, and circles indicate the relative positions of lines-of-sight for radio sources. The radius of the circle represents the solar wind speed. Red circles denote high speed (>1000 km/s) plasma flow. The solar offset distances of high-speed data for November 8-9 (right panel) are larger than those for November 7-8 (left panel). This fact suggests that the expanding CME was approaching near the Earth. The shock in association with the X2.0 flare arrived on Earth at ~09 UT in November 9th.

Figure 11 CME-CME interaction (unused?)

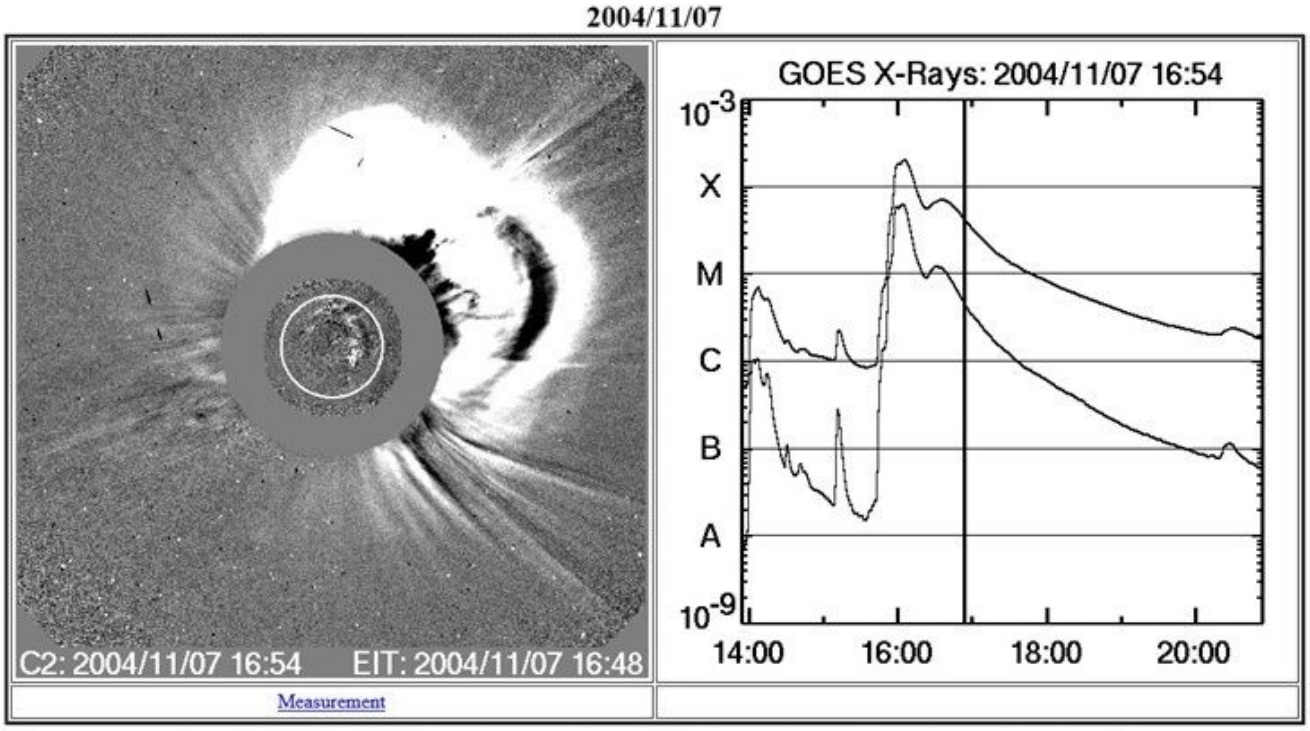

Figure 11

The image of the CME-CME interaction taken by the SOHO LASCO telescope at 16:54 UT on November 7th, 2004. The central white circle represents the solar surface.

Figure 12 SOHO CME data

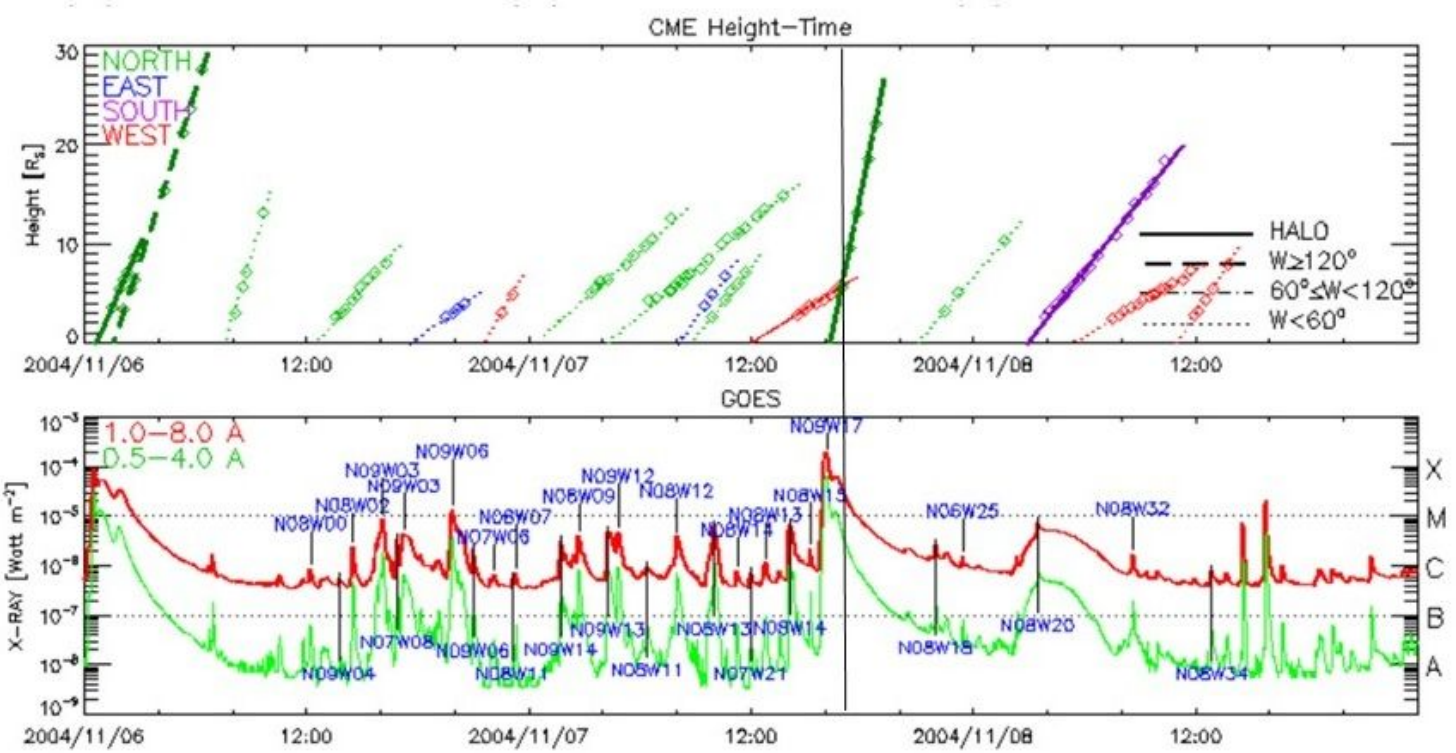

Figure 12

The CME emission log from November 6th 00UT to November 8th 00UT observed by the SOHO coronagraph. Two high speed CMEs are recognized in the plot in association with the two large solar flares at November 6th (at 00:34UT) and November 7th (at 16UT). Before the emission of the CME at 16UT, another CME was emitted around 12UT of November 7th with rather slow speed. As a result, they will collide at 17UT. The collision time is indicated by the vertical line in the figure. The CME emission log is shown together with the GOES X-ray data as reference. The numbers in the GOES X-ray data indicate the flare position on the solar surface. The data are available from SOHO home page.

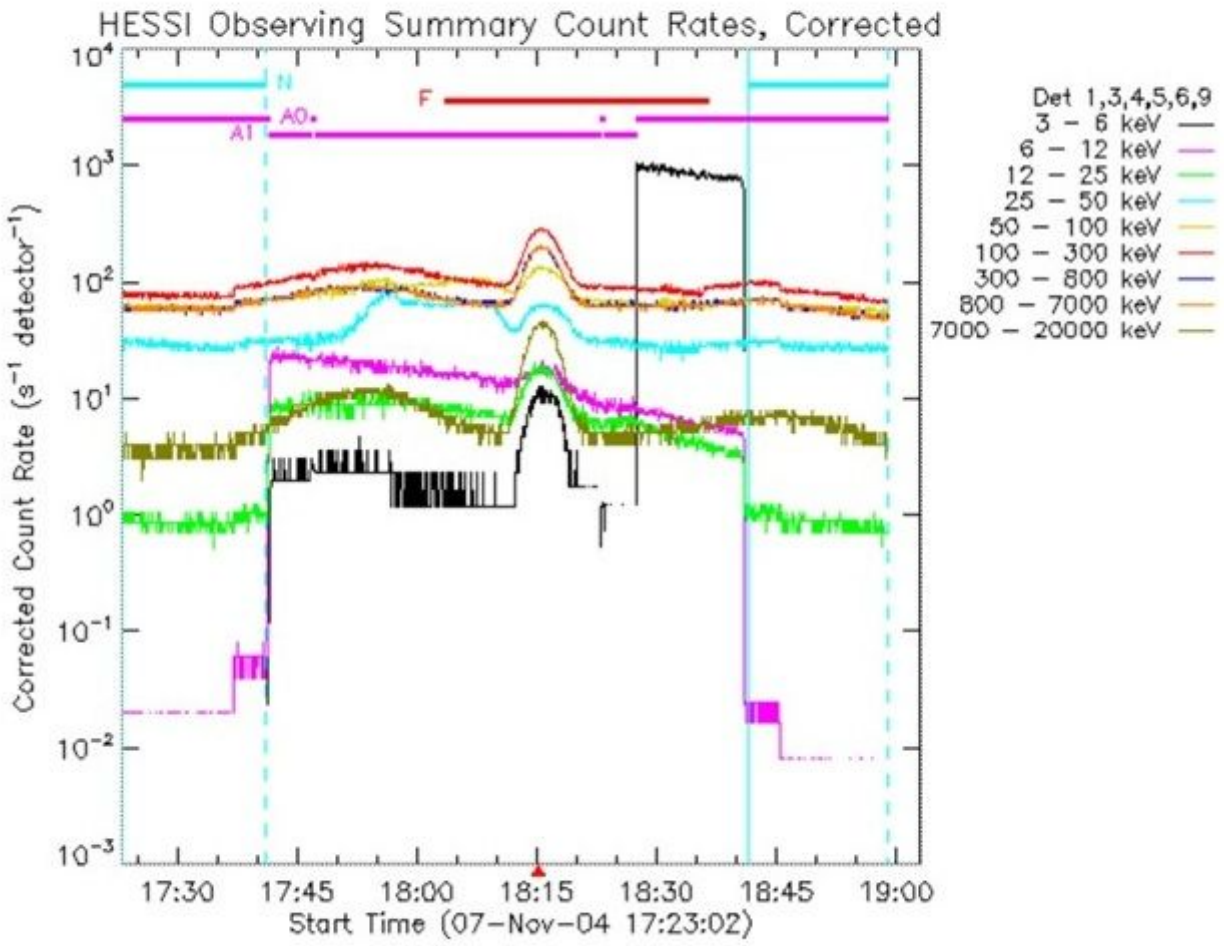

Figure 13

The flux of X-rays observed by the RHESSI satellite. At 18:15 UT a small bump can be recognized.

Supplementary Files

This is a list of supplementary files associated with this preprint. Click to download.

- FiguresfortheJournals.jpg
- graphicalabstract.jpg